HHS Public Access

Author manuscript

Nat Biotechnol. Author manuscript; available in PMC 2015 July 01.

Published in final edited form as:

Nat Biotechnol. 2015 January ; 33(1): 97–101. doi:10.1038/nbt.3104.

Biopolymer implants enhance the efficacy of adoptive T cell therapy

Sirkka B. Stephan[1], **Alexandria M. Taber**[1], **Ilona Jileaeva**[2], **Ericka P. Pegues**[2], **Charles L. Sentman**[3], and **Matthias T. Stephan**[1,2,4,5,‡]

[1]Clinical Research Division, Fred Hutchinson Cancer Research Center, Seattle, Washington, USA

[2]Technology Access Foundation (TAF) Academy, Fred Hutchinson Cancer Research Center, Seattle, Washington, USA

[3]Department of Microbiology and Immunology, The Geisel School of Medicine at Dartmouth, Lebanon, New Hampshire, USA

[4]Department of Bioengineering and Molecular Engineering & Sciences Institute, University of Washington, Seattle, Washington, USA

[5]Department of Medicine, Division of Medical Oncology, University of Washington, Seattle, Washington, USA

Abstract

Although adoptive T cell therapy holds promise for the treatment of many cancers, its clinical utility has been limited by problems in delivering targeted lymphocytes to tumor sites, and their inefficient expansion in the immunosuppressive tumor microenvironment. Here we describe a bioactive polymer implant capable of delivering, expanding and dispersing tumor-reactive T cells. The approach can be used to treat inoperable or incompletely-removed tumors by situating implants near them, or at resection sites. Using a mouse breast cancer resection model, we show that the implants effectively support tumor-targeting T cells throughout resection beds and associated lymph nodes, and reduce tumor relapse compared to conventional delivery modalities. In a multifocal ovarian cancer model, we demonstrate that polymer-delivered T cells trigger regression whereas injected tumor-reactive lymphocytes have little curative effect. Scaffold-based T cell delivery may provide a viable treatment option for inoperable tumors, and reduce the rate of metastatic relapse after surgery.

‡To whom correspondence should be addressed. mstephan@fhcrc.org.

AUTHOR CONTRIBUTIONS

S.B.S. designed and performed experiments and analyzed and interpreted data. A.M.T. helped perform experiments, E.J. and E.P.P. helped prepare scaffolds and microparticles, C.L.S. provided NKG2D CARs constructs, and M.T.S designed the study, performed experiments, analyzed and interpreted data and wrote the manuscript.

COMPETING FINANCIAL INTERESTS

The NKG2D CAR technology used in this paper is licensed by Celdara Medical, LLC. Dr. Sentman and Celdara are developing the technology for clinical use, for which he receives compensation. These activities are in full compliance with the policies of Dartmouth College.

Solid cancers are usually treated surgically, but in some cases resection is dangerous or impractical. Furthermore, surgical approaches risk relapse from residual tumor cells. Treatment with tumor-reactive T cells ("adoptive cell therapy", ACT) is being explored as a means to eradicate tumor lesions that cannot be removed by surgery[1–3], and this approach has yielded promising results for several types of cancer, including melanoma, cervical cancer, and synovial cell sarcoma[4–6]. Unfortunately, the effect of ACT on most solid malignancies is impaired by inefficient trafficking of infused lymphocytes to the tumor, and inadequate T cell expansion in the immunosuppressive tumor microenvironment[7–9]. Thus, there is substantial interest in creating more effective ways to harness the inherent anti-tumor activity of immune cells to treat incompletely resected or inoperable tumors.

Here we demonstrate that the anti-tumor potency of transplanted lymphocytes can be substantially improved by harboring them in bioengineered polymer matrices designed to deliver and stimulate them when placed in tumor resection sites or close to inoperable tumors (Fig. 1a). The polymer acts as an active reservoir from which the propagating cells are released as the material biodegrades (Fig. 1b).

An effective T cell delivery and release platform must support cell egress and provide stimulatory signals to trigger proliferation. We created macroporous scaffolds from polymerized alginate (a moldable, naturally-occurring polysaccharide already FDA-approved because of its biocompatibility and biodegradability[10]). Lymphocytes normally migrate along collagen fibers, so we integrated GFOGER (a synthetic collagen-mimetic peptide (CMP) that binds to lymphocytes via the $\alpha_2\beta_1$ collagen receptor[11]) into the scaffolds using carbodiimide chemistry (Supplementary Fig. 1a, b). Time-lapse microscopy established that T cells migrate through these scaffolds with a velocity similar to those in lymphoid organs (averaging 8.9 μm/min[12]; Fig. 2a; Supplementary Fig. 1c). Thus, in 30 min they travel 119 μm ± 37 μm (Fig. 2b), whereas lymphocytes in unmodified scaffolds only circulate within their void space (mean displacement: 7 μm ± 4.8 μm; Fig. 2a, b; Supplementary Movie 1). CMP contact also increased viability compared with unmodified alginate or plastic (Supplementary Fig. 1d), perhaps reflecting activation of collagen-dependent pro-survival pathways.

We next measured how CMP affected the egress of 4T1 breast tumor-specific lymphocytes (Supplementary Fig. 2) into 3D collagen gels bearing the inflammatory cytokine IP-10 (as a surrogate for natural resection margins; Fig. 2c). In alginate, cells mainly accumulated in void spaces during the seven-day test. Modification with CMP increased cell transit by 6.3-fold (Fig. 2d) and maintained their immune functions, as reflected by cytokine secretion and destruction of 4T1 (but not B16F10 melanoma) targets (Supplementary Fig. 3).

Ideally, lymphocyte-based cancer treatments will duplicate the activation processes normally evoked by signals from antigen-presenting cells, including secreted factors and membrane-bound costimulatory ligands. We integrated porous silica microparticles into scaffold void spaces as a substrate for both kinds of signals (Fig. 2e) because their physical characteristics support high-capacity encapsulation and sustained release of soluble biomolecules, and they can be coated with lipid bilayers to mimic cell membranes[13]. For the soluble factor, we used interleukin 15 superagonist (an IL-15/IL-15Rα fusion protein 50-

fold more potent than native IL-15[14]), which the microparticles harbor and release in a bioactive form (Supplementary Fig. 4). Because receptor-induced lymphocyte proliferation involves synergistic CD28/CD137 signaling[15], we provided membrane-bound ligands by coupling anti-CD3, anti-CD28, and anti-CD137 antibodies to the microsphere bilayers. Adding these particles to GFOGER-modified alginate solutions before casting into 3D scaffolds (Fig. 2e) triggered a 22-fold boost in T cell proliferation and substantially increased migration into the surrounding collagen gel (8.3-fold during the 7-day test period; Fig. 2f). Further analyses revealed amplification of T cell anti-tumor functions (Supplementary Fig. 5) and reduced susceptibility to apoptosis (Fig. 2g). Various tests showed that simultaneous activity of these components maximized the effect (Supplementary Fig. 6). These findings establish that biomaterials augmented with migration-promoting macromolecules and stimulatory cues can serve as efficient delivery vehicles for anti-cancer T cells.

We used the 4T1 mouse breast tumor resection model (which mimics local and systemic recurrences arising post-surgically) to measure the effectiveness of delivering lymphocytes via scaffolds compared with conventional injection. Ten days after introducing luciferase-expressing 4T1 cells into mammary glands, we resected tumors leaving ~1% residual diseased tissue. In the first of six randomly-assigned groups, we implanted scaffolds containing 7×10^6 tumor-reactive T cells directly into the resection cavity (Fig. 1a, middle panel). Two groups received the same T cell dose injected either intravenously or directly into the resection bed. For the fourth group, we pre-activated T cells with IL-15 superagonist and anti-CD3, anti-CD28, and anti-CD137 antibodies *in vitro* prior to local injection. Background effects were measured by implanting mice with acellular scaffolds, and controls received no treatment. Conducting bioluminescence imaging to quantify tumor growth, we found that intravenous injection of T cells prevented metastatic relapse no better than controls (median survival: 21 versus 19 days, respectively; $P = 0.21$, Fig. 3a, b). Injecting cells directly into the resection cavity produced a temporary reduction in residual tumors, yielding a modest (4 day) survival advantage ($P = 0.03$). Time to relapse was further prolonged by pre-activating the injected cells (median survival: 30 days versus 25 days; $P = 0.048$), but did not prevent recurrence. By contrast, none of the animals receiving scaffold-delivered T cells experienced tumor relapse (Fig. 3a, b, Supplementary Fig. 7). Luciferase-negative 4T1 tumors produced the same results (Supplementary Fig. 8). As expected, cell-free scaffolds or those containing non-specific lymphocytes did not produce anti-tumor benefits (Supplementary Fig. 9).

To determine how biomaterial-supported lymphocyte delivery prevents tumor relapse more effectively than cell injections, we transduced 4T1-specific T lymphocytes with click beetle red luciferase (CBR-luc) and tracked their migration and distribution with bioluminescence imaging. We found intravenously injected cells accumulated in the spleen and the liver (Fig. 3c); neither doubling the cell number nor supplementing them with systemic IL-15/IL15Rα injections substantially improved their targeting to tumor sites (Supplementary Fig. 10). Of course, T cells injected directly into the resection cavity were seen there at first, but they persisted poorly (Fig. 3c, Supplementary Fig. 11a–c) and became functionally exhausted (Tim-3^{high}, 2B4^{high}; Supplementary Fig. 11d). By contrast, scaffold-delivered T cells

proliferated at the resection site (167-fold higher relative to injected pre-stimulated T cells, $P < 0.0001$; Fig. 3c, Supplementary Fig. 12). Flow cytometry and lymphocyte counts confirmed that our recorded bioluminescent signals accurately reflect cell numbers in the resection bed (Supplementary Fig. 13). We also conducted confocal microscopy to confirm substantial infiltration of material-deployed T cells into peritumoral tissue (Fig. 3d). Despite their high proliferation rate, delivered cells maintained a non-exhausted (i.e. Tim-3^{low}, $2B4^{low}$) phenotype (Supplementary Fig. 11). T cells egressing from implants also populated tumor-draining lymph nodes (54-fold higher levels than injected pre-stimulated cells, $P < 0.0001$; Fig. 3c, Supplementary Fig. 14a, b), where they acquired a $CD44^+$ $CD62L^+$ central memory phenotype (Supplementary Fig. 14c, d). Notably, removal of endogenous lymphocytes by cyclophosphamide pre-treatment did not affect the results (Supplementary Fig. 15).

To measure how scaffold-delivered lymphocytes affect advanced-stage unresectable tumors, we developed a model of stage 3 ovarian carcinoma (which has extensive peritoneal metastases) based on ID8 tumor cells expressing vascular epithelial growth factor (VEGF) to promote tumor growth[16]. Incorporation of VEGF-A makes this model more aggressive[16], more immunosuppressive[17], and more representative of human ovarian tumors that express the VEGF gene (and consequently often have a poor prognosis). Developing in immune-intact animals over eight weeks, the model involves extensive infiltration by myeloid and lymphoid cells[18]. ID8-VEGF provides a better test for the treatment of inoperable tumors than e.g. ID8 inoculation into the ovarian bursa, or p53-dependent KRAS-induced spontaneous ovarian tumors[19], as these usually develop lesions like those routinely resected via salpingo-oophorectomy.

Our model uses C57BL/6 mice which, being albino (due to a tyrosinase mutation), do not suffer pigmentation-related signal losses (note that tyrosinase is not expressed by ID8-VEGF tumor cells (Supplementary Fig. 16a) and has no known role in ovarian cancer). Two months after intraperitoneal inoculation, tumor nodules occur throughout the peritoneal wall and intestinal mesentery of these mice (Fig. 3e, Supplementary Fig. 16b, c). Without therapy, they develop features of advanced serous ovarian cancer (e.g., bloody ascites and peritoneal carcinomatosis; Supplementary Fig. 16d). When we implanted T cells expressing a chimeric natural killer receptor (consisting of NKG2D linked to the cytoplasmic signaling domain of CD3ζ[20]) specific for Rae-1 (an antigen characterizing ID8 (and ID8-VEGF) cells; Supplementary Fig. 17), disseminated tumors were eradicated in six of ten mice (Fig. 3e, f). The remaining four showed substantial tumor regression (and had an average 27-day improvement in survival; Fig. 3f, Supplementary Fig. 18). Locally injected T cells never produced complete tumor clearance, nor did they expand in number (Fig. 3g, h, Supplementary Fig. 19), unlike scaffold-delivered cells which proliferated vigorously in the peritoneal cavity (98-fold higher than injected pre-stimulated cells after 12 days, $P < 0.0001$; Fig. 3g, h).

These results indicate that launching cancer-fighting T cells from polymeric devices may provide an effective therapy for incompletely resected or inoperable tumors. Biomaterials have been used before to supply cells for tissue repair, and antigens to elicit immune responses[21–23], but to the best of our knowledge this ours is the first use of them to deliver

anti-tumor lymphocytes to rapidly destroy tumors (Fig. 3a, e). This approach could help resolve two issues that currently limit the implementation of lymphocyte-based immunotherapies for solid tumors:

First, efficiency. Systemically infusing large numbers of tumor-reactive lymphocytes to treat solid malignancies is rarely curative because they fail to accumulate at the tumor, and fail to expand in the hostile tumor milieu[24, 25]. Our results establish that biodegradable scaffolds can overcome the immunosuppressive barriers created by tumors, and gradually disperse the proliferating anticancer T cells they harbor throughout the tumor bed (Fig. 3d–f).

Second, practicality. Adoptive cell therapy is an elaborate procedure: lymphocytes must be isolated from the patient and expanded in specialized *in vitro* facilities–a costly and time-consuming procedure that can functionally exhaust cells before they are reintroduced[26]. ACT also requires conditioning regimens like irradiation, lymphodepleting chemotherapy, and/or cytokine support[27]. In our approach, activation and proliferation factors are incorporated into the scaffold, the lymphocytes can act on residual cancer immediately because migration is unnecessary and host lymphodepletion is not required. Thus, scaffold delivery may minimize side effects and facilitate swift patient recovery.

Biomaterial-supported T-cell implants, as a form of localized immunotherapy, are not primarily designed to treat widespread tumor metastases in liver or lung (where T cells tend to passively accumulate following intravenous injection). Our goal was to address locally advanced, unresectable or incompletely resected tumors (e.g., pancreatic and ovarian cancer, brain tumors, sarcomas, mesothelioma, and advanced breast cancer). That said, it is possible that biopolymer scaffolds could evoke antitumor immune responses capable of eliminating widespread tumor metastases. We are currently testing this by incorporating slow-release depots of vaccine adjuvants into T cell-loaded scaffolds as a means to launch systemic antitumor immunity.

Besides T lymphocytes, this platform could easily be adapted to deliver other tumor-fighting immune cells, such as natural killer or invariant NKT cells, or even synergistic cell combinations. It is also amenable to cells that are difficult to expand *ex vivo* or that require tightly controlled microenvironments (like type 1 T-helper cells or stem cell-like memory T cells). Likewise, supplements to support cell function or offset tumor suppression could be delivered by the scaffolds. For example, the anti-CTLA-4 immune checkpoint inhibitor significantly prolongs relapse-free survival in some cancer patients, but fails to reject residual disease in mice following 4T1 breast tumor resection (Supplementary Fig. 20). Incorporation of slow-release repositories of anti-CTLA-4 into T cell-loaded scaffolds could amplify their anti-tumor effector functions and, at the same time, activate host lymphocytes to destroy dispersed cancer cells. By focusing drug actions on the intended target cells, this delivery device may maximize their performance while avoiding toxic side effects.

In summary, our findings establish that appropriately-designed polymer delivery systems can substantially improve the ability of anticancer immune cells to eradicate tumors. Implemented in the clinic as an intraoperative tool, biomaterial-supported T cell implants could maximize the success of surgical interventions and offer an alternative option to

patients who have inoperable tumors. Beyond its potential for cancer therapy, this technology may inspire new treatments that involve localized, sustained release of cells and bioactive molecules.

METHODS

Cell lines

The murine 4T1 breast cancer and B16F10 melanoma cell lines (American Type Culture Collection) were cultured in complete RPMI 1640 medium with 10% heat-inactivated fetal bovine serum (FBS), 2 mM L-glutamine, 1.5 g/L sodium bicarbonate, 4.5 g/L glucose, 10 mM HEPES, 1.0 mM sodium pyruvate, and 0.05 mM 2-mercaptoethanol.

The murine ovarian cancer cell line ID8, a gift from Dr. Katherine Roby (University of Kansas Medical Center, Kansas City, KS), was cultured in DMEM supplemented with 4% FBS and 5 μg/ml insulin, 5 μg/ml transferrin, and 5 ng/ml sodium selenite (all Sigma-Aldrich). To generate the more aggressive Vascular Endothelial Growth Factor (VEGF)-expressing ID8 strain, we transfected ID8 tumor cells with the pUNO1 plasmid (Invivogen) encoding murine VEGF and the blasticidin-resistance gene. To obtain stable transfectants, tumor cells were cultured in complete medium containing 10 μg/ml Blasticidin (Invivogen) for three weeks. The Phoenix™ Eco retroviral packaging cell line (Orbigen) was cultured in DMEM containing 10% FBS, 2 mM glutamate, 100 U/mL penicillin, and 100 μg/mL streptomycin. For *in vivo* bioluminescent imaging, the 4T1 and ID8-VEGF cell lines were retrovirally transduced with firefly luciferase (F-luc). We also generated a 4T1 tumor cell line that expresses the costimulatory ligands B7.1 and 4-1BBL (4T1 B7.1/4-1BBL) to expand breast tumor-specific T cells *ex vivo*. For experiments involving confocal imaging, we retrovirally transduced 4T1 cells with green fluorescent protein.

Mice and *in vivo* tumor models

Animals were housed in the animal facility of Fred Hutchinson Cancer Research Center, and used in the context of an animal protocol approved by their Institutional Animal Care and Use Committee. Female BALB/cJ mice (4–6 weeks old) were obtained from Jackson Laboratories (Stock # 000651). We generated the 4T1 tumor-specific T cells in BALB/c mice that are congenic for the CD45.1 marker (CBy.SJL(B6)-*Ptprca*/J), to distinguish them from host lymphocytes in the experimental BALB/c mice (which were congenic for CD45.2). To measure effects on relapse, ten days after 1×10^6 luciferase-tagged 4T1 tumor cells were transplanted into the mammary gland, tumors were resected leaving ~1% residual tissue behind, and 7×10^6 effector $CD8^+$ T cells were administered immediately afterwards. For the advanced-stage ovarian tumor model, 5×10^6 ID8-VEGF tumor cells were injected intraperitoneally into female Albino B6 (C57BL/6J-Tyr<c-2J>) mice (Jackson Laboratories) and were allowed to establish for eight weeks. Mice were then treated with 7×10^6 T cells genetically modified with chimeric NKG2D receptors (NKG2D CARs). With the exception of experiments in Supplementary Fig. 15, all mice were preconditioned with 100 mg/kg cyclophosphamide intraperitoneally to eliminate endogenous lymphocytes a day before T-cell transfer.

Retroviral vectors and viral production

SFG-CBR-luc (expressing click beetle red luciferase), SFG-F-luc (expressing firefly luciferase), and SFG-B7.1 and SFG-4-1BBL (encoding the costimulatory ligands B7.1 and 4-1BBL) vectors were kindly povided by Dr. Michel Sadelain (Memorial Sloan-Kettering Cancer Center, New York). The retroviral vector pFb-chNKG2D-IRES-Neo was provided by Dr. Charles Sentman (The Geisel School of Medicine at Dartmouth, Lebanon). NKG2D CARs consist of the full-length mouse NKG2D fused with the cytoplasmic portion of CD3ζ. To generate retroviral particles, Phoenix Eco cells (1.5×10^6/10 cm culture plate) were transfected overnight with 10 μg of vector-DNA using standard calcium phosphate methods; the following day, they were incubated in 10 mL fresh DMEM for an additional day before the retroviral supernatant was filtered (0.45-μm, Nalgene) and concentrated 10-fold using Ultracel 100K membranes (Millipore).

Preparation of tumor-targeting lymphocytes

We primed breast tumor-specific T cells by immunizing BALB/c mice with 4×10^6 irradiated (200 Gy) 4T1 B7.1/4-1BBL tumor cells (along with the adjuvants CpG oligodeoxynucleotide and Poly(I:C)) one day after preconditioning them with 50 mg/kg cyclophosphamide. Booster injections were administered after 30 days. Six days later, inguinal lymph nodes and spleens were digested into cell suspensions for co-culture on irradiated 4T1 B7.1/4-1BBL monolayers in the presence of 10 ng/mL exogenous interleukin (IL)-2 and IL-15. We removed dead cells 7 days later by centrifugation through a Ficoll gradient (GE Healthcare), then isolated $CD8^+$ cells using a mouse CD8 Negative Isolation Kit (Stemcell Technologies). These T cells were used for treatments the same day. To generate ovarian cancer-specific (NKG2D CAR-transduced) T cells, spleens of C57BL/6J mice were harvested, macerated over a filter, and resuspended in ACK lysing Buffer (Biosource). Effector $CD8^+$ T cells were prepared by incubating splenocytes (3×10^6/mL) in complete RPMI 1640 with 1 ng/mL interleukin-7 (PeproTech) and 2 μg/mL Concavalin A (Calbiochem) at 37°C. Two days later, dead cells were removed by Ficoll gradient separation (GE Healthcare) and $CD8^+$ cells were isolated using a mouse CD8 Negative Isolation Kit (Stemcell Technologies). Introduction of the NKG2D CAR into T cells was performed by retroviral transduction. Concentrated NKG2D CAR expressing retrovirus (1 mL) was preloaded onto six-well non-tissue culture treated dishes coated with RetroNectin (TakiraBio) and incubated at 37°C for 1 hr. An equal volume of isolated T-cells (3×10^6 cells/mL supplemented with 10 ng mIL-2/mL) was added and centrifuged at 2000 × g for 30 min). 6 hr after spinoculation, 1 mL of fresh, prewarmed RPMI, containing 10 ng mIL-2 (PeproTech) was added. Two days after infection, transduced primary T cells ($0.5–1 \times 10^6$/mL) were selected in RPMI-10 media containing G418 (0.5 mg/mL) plus 25 U/mL recombinant human (rHu) IL-2 for an additional 3 days. Viable cells were isolated using Histopaque-1083 (Sigma, St Louis, MO) and expanded for 2 days without G418 before adoptive transfer.

For bioluminescence T-cell imaging experiments, the targeted T cells were genetically tagged with click beetle red luciferase (CBR-luc). Six hours after this spinoculation, 1 mL of RPMI containing 50 IU IL-2 was added, and the transduced T cells were used for experiments 1 day later.

To treat mice with ex vivo prestimulated T cells, we coated six-well non-tissue culture treated dishes overnight with a cocktail of anti-mouse CD3, CD28, and CD137 antibodies (BioXcell) at a concentration of 10 μg/mL. Plates were then washed with sterile PBS, and 7 × 10^6 T cells supplemented with 70 ng/mL IL-15/IL-15Rα fusion protein were added. Twelve hours after stimulation T cells were used for adoptive transfer.

Recombinant IL-15/IL-15Rα protein expression and production

We generated a pDisplay Vector (Life Technologies) encoding His-tagged IL-15/IL-15Rα (IL-15 linked to IL-15P sushi)[28]. Following transfection of 293-F cells, we purified protein from culture supernatant using standard Cobalt agarose resin (Thermo Scientific) according to protocol.

Preparation of stimulatory lipid-coated silica microspheres

Preparation of maleimide-functionalized lipid film—Lipid stock solutions were formulated in chloroform. 140 μL DOPC (10 mg/mL), 30 μL DSPE-PEG(2000) maleimide (5 mg/mL), 150 μL cholesterol (5 mg/mL), and 50 μL 18:1 PEG 2000-PE (5 mg/mL, all purchased from Avanti Polar Lipids) were combined to attain a DOPC:DSPE-PEG(2000) maleimide:cholesterol:PEG 2000-PE mass ratio of 55:5:30:10 and 2.5 mg total lipid. Chloroform was evaporated under a stream of nitrogen and residual solvent was removed under vacuum overnight.

Loading of cytokine into mesoporous silica microparticles—A 100 mg/mL suspension of spherical silica (SiO_2) gel (15 μm particle diameter, 100 Å pore diameter, Sorbent Technologies) was prepared in phosphate buffered saline at pH 7.2 (PBS), and 120 μL of it was combined with 400 μL of IL-15/IL-15Rα fusion protein (22 μg/mL), gently vortexed for 1 h, then diluted with 480 μL PBS.

Lipid adsorption on silica—The entire SiO_2/IL-15/IL-15Rα suspension (1 mL) was added to a 2.5 mg batch of lipid film and vortexed for 15 s at 10 min intervals for a total of 1 h. The particles were pelleted at 3500 × g for 2 min, washed with PBS (3 × 1 mL), then resuspended in 500 μL PBS.

Antibody conjugation to lipid-coated microparticles—The hinge region disulfide bonds of anti-mouse CD3, CD28, and CD137 antibodies (BioXcell) were selectively reduced with dithiothreitol (DTT). After DTT was removed with a desalting column, these mildly-reduced antibodies (anti-CD3: 200 μg; anti-CD28 and CD137: 400 μg) were added to maleimide-functionalized particles, vortexed briefly before rotation for 2 h, and centrifuged at 3500 × g for 2 min. The pellet was washed with PBS (3 × 1 mL), then suspended in 125 μL PBS.

Scaffold fabrication

We produced the alginate scaffolds from high molecular weight (~250 kDa) ultrapure sodium alginate powder (Novamatrix Pronova UP MVG alginate) enriched in G blocks (≥ 60%) after it was oxidized with sodium periodate to create hydrolytically labile bonds, as previously described[29]. Briefly, 200 μL of 0.25% sodium periodate was added dropwise to

10 mL aqueous 1% alginate, and stirred in the dark at 25°C for 5 h before the reaction was quenched by stirring with equimolar ethylene glycol for 30 min. The sample was dialyzed against deionized water for three days using membranes with a 3,500 molecular weight cut-off, then lyophilized. The oxidized alginate solution was reconstituted in a MES solution (0.1 M MES, 0.3 M NaCl, pH 6.5) and covalently conjugated to the collagen-mimetic peptide GFOGER[11] (obtained from the MIT Biopolymers facility) using carbodiimide chemistry: sulfo-NHS, EDC (both Thermo Scientific), and the GFOGER peptide were added sequentially, and 24 h later the solution was again dialyzed (MWCO 20 kDa dialysis membrane, Thermo Scientific) and lyophilized.

To make scaffolds, the alginate stock was reconstituted to 7 mL of a 2% w/v solution in PBS, and warmed to 55 °C before mixing with 7×10^6 stimulatory microspheres in aqueous suspension. Mild cross-linking was initiated by adding 1.4 mL of 0.1% (w/v) calcium chloride solution while vortexing, then 700 μL was immediately transferred per 15 mm round Teflon-coated mold to form 2 mm-thick scaffolds. These were frozen at −78 °C and lyophilized to yield porous matrices, which were stored at 4 °C in a desiccator.

T cell seeding onto scaffolds

Following *ex vivo* expansion, mouse $CD8^+$ effector T cells specific for 4T1 breast tumor antigens or genetically engineered to express NKG2D-CAR were washed twice in PBS and resuspended in non-supplemented RPMI medium at a concentration of 14×10^6 cells/mL. After adding 5% AlgiMatrix Firming Buffer (Invitrogen), 500 μL of this cell suspension was immediately inoculated on top of each lyophilized scaffold in a 24-well tissue culture plate. Cells were allowed to infuse into these matrices on ice for 30 min before implantation into the tumor resection cavity or the peritoneal cavity.

Functional *in vitro* T cell assays

T cell migration studies—T cell-loaded scaffolds were monitored with a Nikon Eclipse Ti inverted time-lapse microscope equipped with a humidified environmental chamber (37°C, 5% CO_2), and images were collected with a digital CCD camera (CoolSnap HQ, Photometrics) using Prairie View software (Prairie Technologies). To track single-cell migration, time-lapse images were collected at 30 s intervals for 30 min using a 40× N.A. 1.3 oil immersion objective. Maximum projections of brightfield image stacks were computed with Prairie View software. In each of two independent experiments, movements of 30 T cells were quantitatively tracked using Volocity software (Improvision).

T-cell release assay—We measured the egress of lymphocytes from scaffolds by abutting them to a three-dimensional 3.0 mg/mL collagen gel (PureCol) containing 10 ng/mL inflammatory cytokine IP-10 and culturing in complete RPMI medium. At selected experimental time points, cells were separately recovered from scaffolds and collagen gels using Algimatrix dissolving buffer (Invitrogen) or collagenase enzyme digestion, respectively. The number of viable T cells in each was determined by Trypan Blue exclusion.

Cytotoxicity assays—We measured *in vitro* cytotoxic activity of T cells using standard ^{51}Cr release assays as described elsewhere[30]. Briefly, 4T1 breast tumor, ID8-VEGF ovarian tumor or B16F10 melanoma control tumor cells were labeled with ^{51}Cr for 1 h at 37°C, washed with RPMI containing 10% FCS, and resuspended in the same medium at a concentration of 1×10^5 tumor cells/mL. T cells were added to the suspensions at varying effector-to-target cell ratios in 96-well plates (final volume, 200 μL) and incubated for 4 h at 37°C, then 30 μL of supernatant from each well was transferred into Lumaplate-96 microplates (Packard Bioscience) for analysis with a Top Count NXT microplate scintillation counter (Packard Bioscience). Effector cell numbers were calculated based on the total number of IFN-γ^+ CD8$^+$ T cells measured by flow cytometry using commercially available kits (R&D Systems).

Intracellular IFN-γ assay—To determine the percentage of 4T1 breast tumor-specific T cells before and after *ex vivo* expansion, we cocultured the lymphocytes on irradiated 4T1 B7.1/4-1BBL monolayers in the presence of 5 μg/mL brefeldin A for 12 h, then measured intracellular IFN-γ by flow cytometry.

Cytokine secretion assays—T cell cytokine release was measured with ELISA (R&D Systems) 24 h (IL-2) or 48 h (IFN-γ and TNF-α) after stimulation on irradiated 4T1 B7.1/4-1BBL monolayers.

In vivo bioluminescence and imaging

We used D-Luciferin (Xenogen) in PBS (15 mg/mL) as a substrate for F-luc (imaging of 4T1 breast tumor and ID8-VEGF ovarian tumor) and CBR-luc (T-cell imaging). Bioluminescence images were collected with a Xenogen IVIS Spectrum Imaging System (Xenogen, Alameda, CA). Living Image software version 4.3.1 (Xenogen) was used to acquire (and later quantitate) the data 10 min after intraperitoneal injection of D-luciferin into animals anesthetized with 150 mg/kg of 2% isoflurane (Forane, Baxter Healthcare). Acquisition times ranged from 10 sec to 5 min.

Adjuvant therapy with anti-CTLA-4 antibodies or Paclitaxel

Following incomplete breast tumor resection, animals were treated with intraperitoneal injections of anti-CTLA-4 antibody (clone 9H10, BioXCell, 100 μg/dose) or Taxol (Paclitaxel, Tocris Bioscience, 5 mg/kg in DMSO) every three days for a maximum of 30 days.

Adjuvant IL-15/IL-15Rα cytokine therapy

For experiments in Supplementary Figure 10, 2 ug IL-15/IL-15Rα protein was freshly reconstituted in PBS and administered by i.p. injection twice daily, beginning the day of adoptive transfer, for 3 d. The initial cytokine dose was co-injected i.v. with adoptively transferred T cells.

Flow cytometry

Anti-recombinant Annexin V (used to quantify apopotic cells) and other antibodies used with the FACSCanto Flow Cytometer (BD Biosciences) were purchased from eBioscience.

Confocal microscopy

To visualize scaffolds by confocal microscopy, we conjugated Hilyte Fluor 647 (Anaspec) to alginate using standard EDC/NHS chemistry, then mixed 1 part of the conjugate with 9 parts of GFOGER-modified alginate to fabricate scaffolds as described above. T cells were labeled with CellTracker Orange CMTMR (Invitrogen) immediately before seeding into these scaffolds. Three days post-implantation, the tumor resection bed was snap-frozen in OCT (Tissue-Tek) to produce cryosections, which were fixed with 2% paraformaldehyde, mounted in ProLong Gold Antifade reagent (Invitrogen), and imaged with a Zeiss LSM 780 NLO laser scanning confocal microscope.

Statistical methods

Statistical significance of measured differences in T cell migration parameters was calculated using one-way ANOVA, followed by Dunnett's comparison test. Pairwise differences in the bioluminescent tumor and T cell signals were analyzed at selected time points using the Wilcoxon rank-sum test, and we characterized survival data using the Log-rank test. All statistical analyses were performed using GraphPad Prism software version 6.0.

Supplementary Material

Refer to Web version on PubMed Central for supplementary material.

Acknowledgments

We thank David Ehlert (cognitionstudio.com) for the design of the illustration in Fig. 1. This work was supported in part by the Fred Hutchinson Cancer Research Center's Immunotherapy Initiative with funds provided by the Bezos Family Foundation, the NCI (RO1 CA181413), the George and Margaret McLane Foundation, the Breast Cancer Development Research Program funded by the Safeway Foundation and the Seattle Cancer Consortium Breast SPORE (NCI P50 CA138293, PI: Peggy Porter), and the Pacific Ovarian Cancer Research Consortium (NCI P50 CA83636, PI: Nicole Urban).

References

1. Tran E, et al. Cancer immunotherapy based on mutation-specific CD4+ T cells in a patient with epithelial cancer. Science. 2014; 344:641–645. [PubMed: 24812403]
2. Krebs S, Rodriguez-Cruz TG, Derenzo C, Gottschalk S. Genetically modified T cells to target glioblastoma. Frontiers in Oncology. 2013; 3:322. [PubMed: 24427741]
3. Kandalaft LE, Powell DJ Jr, Coukos G. A phase I clinical trial of adoptive transfer of folate receptor-alpha redirected autologous T cells for recurrent ovarian cancer. Journal of Translational Medicine. 2012; 10:157. [PubMed: 22863016]
4. Rosenberg SA, et al. Durable complete responses in heavily pretreated patients with metastatic melanoma using T-cell transfer immunotherapy. Clinical Cancer Research : an official journal of the American Association for Cancer Research. 2011; 17:4550–4557. [PubMed: 21498393]
5. Robbins PF, et al. Tumor regression in patients with metastatic synovial cell sarcoma and melanoma using genetically engineered lymphocytes reactive with NY-ESO-1. Journal of Clinical Oncology : official journal of the American Society of Clinical Oncology. 2011; 29:917–924. [PubMed: 21282551]
6. Hinrichs CS, et al. HPV-targeted tumor-infiltrating lymphocytes for cervical cancer. J Clin Oncol. 2014; 32(5s):abstr LBA3008.

7. Kershaw MH, et al. A phase I study on adoptive immunotherapy using gene-modified T cells for ovarian cancer. Clinical Cancer Research : an official journal of the American Association for Cancer Research. 2006; 12:6106–6115. [PubMed: 17062687]
8. Yaghoubi SS, et al. Noninvasive detection of therapeutic cytolytic T cells with 18F-FHBG PET in a patient with glioma. Nature Clinical Practice Oncology. 2009; 6:53–58.
9. Lamers CH, et al. Treatment of metastatic renal cell carcinoma with CAIX CAR-engineered T cells: clinical evaluation and management of on-target toxicity. Molecular Therapy : the journal of the American Society of Gene Therapy. 2013; 21:904–912. [PubMed: 23423337]
10. Baldwin AD, Kiick KL. Polysaccharide-modified synthetic polymeric biomaterials. Biopolymers. 2010; 94:128–140. [PubMed: 20091875]
11. Wojtowicz AM, et al. Coating of biomaterial scaffolds with the collagen-mimetic peptide GFOGER for bone defect repair. Biomaterials. 2010; 31:2574–2582. [PubMed: 20056517]
12. Miller MJ, Wei SH, Cahalan MD, Parker I. Autonomous T cell trafficking examined in vivo with intravital two-photon microscopy. Proceedings of the National Academy of Sciences of the United States of America. 2003; 100:2604–2609. [PubMed: 12601158]
13. Mamaeva V, Sahlgren C, Linden M. Mesoporous silica nanoparticles in medicine--recent advances. Advanced Drug Delivery Reviews. 2013; 65:689–702. [PubMed: 22921598]
14. Rubinstein MP, et al. Converting IL-15 to a superagonist by binding to soluble IL-15R{alpha}. Proceedings of the National Academy of Sciences of the United States of America. 2006; 103:9166–9171. [PubMed: 16757567]
15. Maus MV, et al. Ex vivo expansion of polyclonal and antigen-specific cytotoxic T lymphocytes by artificial APCs expressing ligands for the T-cell receptor, CD28 and 4-1BB. Nature Biotechnology. 2002; 20:143–148.
16. Janat-Amsbury MM, Yockman JW, Anderson ML, Kieback DG, Kim SW. Comparison of ID8 MOSE and VEGF-modified ID8 cell lines in an immunocompetent animal model for human ovarian cancer. Anticancer Research. 2006; 26:2785–2789. [PubMed: 16886597]
17. Conejo-Garcia JR, et al. Tumor-infiltrating dendritic cell precursors recruited by a beta-defensin contribute to vasculogenesis under the influence of Vegf-A. Nature Medicine. 2004; 10:950–958.
18. Charles KA, et al. The tumor-promoting actions of TNF-alpha involve TNFR1 and IL-17 in ovarian cancer in mice and humans. The Journal of Clinical Investigation. 2009; 119:3011–3023. [PubMed: 19741298]
19. Scarlett UK, et al. Ovarian cancer progression is controlled by phenotypic changes in dendritic cells. The Journal of Experimental Medicine. 2012; 209:495–506. [PubMed: 22351930]
20. Sentman CL, Meehan KR. NKG2D CARs as cell therapy for cancer. Cancer Journal. 2014; 20:156–159.
21. Ali OA, Emerich D, Dranoff G, Mooney DJ. In situ regulation of DC subsets and T cells mediates tumor regression in mice. Science Translational Medicine. 2009; 1:8ra19.
22. Kauer TM, Figueiredo JL, Hingtgen S, Shah K. Encapsulated therapeutic stem cells implanted in the tumor resection cavity induce cell death in gliomas. Nature Neuroscience. 2012; 15:197–204. [PubMed: 22197831]
23. Hori Y, Winans AM, Huang CC, Horrigan EM, Irvine DJ. Injectable dendritic cell-carrying alginate gels for immunization and immunotherapy. Biomaterials. 2008; 29:3671–3682. [PubMed: 18565578]
24. Pule MA, et al. Virus-specific T cells engineered to coexpress tumor-specific receptors: persistence and antitumor activity in individuals with neuroblastoma. Nature Medicine. 2008; 14:1264–1270.
25. Peres E, et al. High-dose chemotherapy and adoptive immunotherapy in the treatment of recurrent pediatric brain tumors. Neuropediatrics. 2008; 39:151–156. [PubMed: 18991194]
26. Tumeh PC, et al. The impact of ex vivo clinical grade activation protocols on human T-cell phenotype and function for the generation of genetically modified cells for adoptive cell transfer therapy. J Immunother. 2010; 33:759–768. [PubMed: 20842061]
27. Rosenberg SA. Cell transfer immunotherapy for metastatic solid cancer--what clinicians need to know. Nature Reviews Clinical Oncology. 2011; 8:577–585.

28. Stone JD, Chervin AS, Schreiber H, Kranz DM. Design and characterization of a protein superagonist of IL-15 fused with IL-15Ralpha and a high-affinity T cell receptor. Biotechnology Progress. 2012; 28:1588–1597. [PubMed: 22961781]

29. Boontheekul T, Kong HJ, Mooney DJ. Controlling alginate gel degradation utilizing partial oxidation and bimodal molecular weight distribution. Biomaterials. 2005; 26:2455–2465. [PubMed: 15585248]

30. Erskine CL, Henle AM, Knutson KL. Determining optimal cytotoxic activity of human Her2neu specific CD8 T cells by comparing the Cr51 release assay to the xCELLigence system. J Vis Exp. 2012:e3683. [PubMed: 22895471]

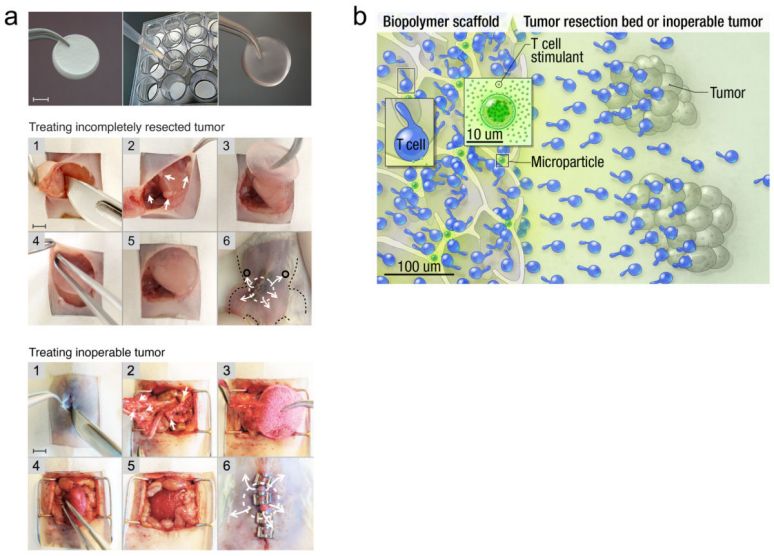

Figure 1.

Biomaterial carriers can deliver anticancer T cells to prevent recurrence or eliminate inoperable tumors. (**a**) Implementation of the approach: The top panel shows hydrating and loading the biopolymer scaffold with tumor-reactive T cells. Scale bar: 0.5 cm. In the middle panel, the loaded device is surgically implanted at a mouse 4T1 mammary tumor resection site to eradicate residual disease there: [1] resection of the tumor; [2] resection cavity with residual tumor tissue; [3–5] implantation of the scaffold; [6] sustained release of tumor-reactive T cells into the resection bed and associated lymph nodes (black circles). Scale bar: 0.5 cm. In the lower panel, a T cell/polymer scaffold is placed directly into the peritoneal cavity to treat disseminated ovarian tumor lesions that cannot be removed by surgery: [1] skin incision; [2] established mouse ID8-VEGF-Luc ovarian cancer metastases (white arrows); [3–5] implantation of T cell-loaded device; [6] dispersion and functional support of anti-tumor T cells throughout the abdominal cavity. Scale bar: 0.5 cm. (**b**) Schematic diagram of a T cell-loaded scaffold surgically situated at a tumor site. Stimulatory microspheres incorporated into the device trigger cell expansion and promote their egress into surrounding tissue.

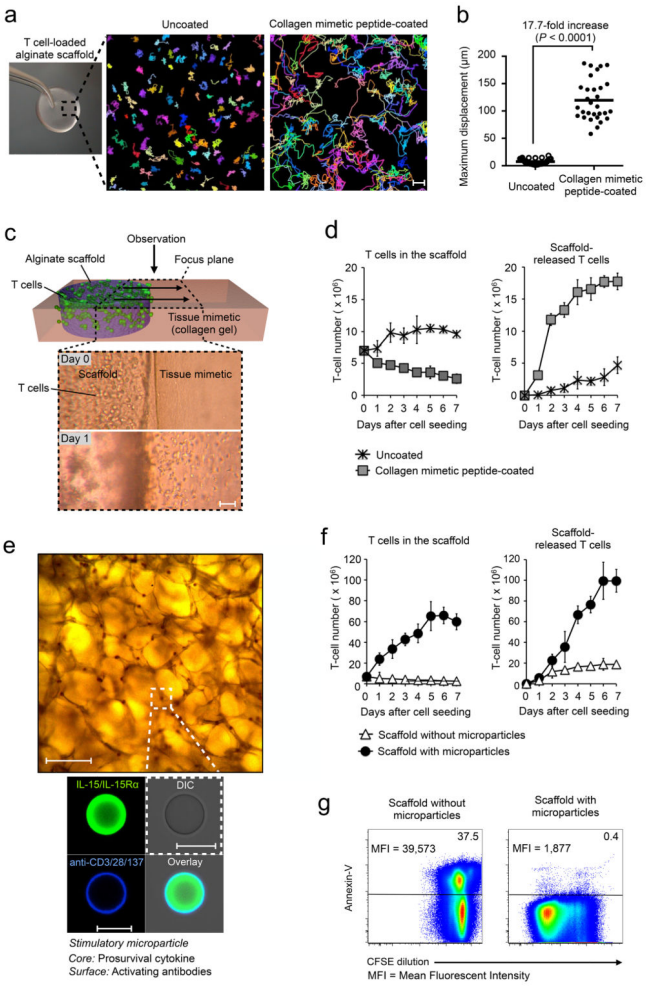

Figure 2.

Porous polysaccharide scaffolds functionalized with appropriate adhesion molecules and stimulatory cues support rapid migration, robust expansion, and sustained release of T cells. (**a**) Time-lapse video projections of lymphocyte migration through uncoated (left) and collagen mimetic peptide (CMP)-coated (right) macroporous alginate scaffolds tracked for 30 min; each color represents an individual T cell. Scale bar: 50 μm. (**b**) Comparison of maximum T cell displacements, based on 30 randomly chosen cells from two independent experiments. (**c–d**) CMP coating promotes the egress of T cells into surrounding tissue: (**c**) Schematic and corresponding micrographs of the *in vitro* assay used to quantify cell migration out of the scaffold (purple) into a tissue mimetic (three-dimensional fibrillar collagen gel; pink). Scale bar: 100 μm. (**d**) Quantification of viable (trypan blue-excluding) T cells enzymatically recovered from scaffolds versus collagen matrices at indicated time points. (**e–g**) Incorporating stimulatory microspheres into matrices amplifies T cell expansion and release: (**e**) Microscopy of scaffolds containing embedded particles. Scale bar: 150 μm. The high magnification confocal images in the *lower panel* show a single lipid-enveloped mesoporous silica microsphere with IL-15/IL15Rα cytokine (Alexa 488-labeled: green) entrapped in the polymer core and stimulatory anti-CD3/CD28/CD137 antibodies (Alexa 647-labeled: blue) tethered to its phospholipid membrane. Scale bar: 15 μm. (**f)**

Absolute counts of viable T cells in scaffolds fabricated with or without stimulatory microparticles (*left panel*), and of cells transited from these implants into surrounding collagen matrix (*right panel*). (**g**) Representative carboxyfluorescein succinimidyl ester (CFSE) assay of T cells that have exited scaffolds during the 7d test period, in which proliferation was assessed by measuring CFSE dilution (consequent to cell division) using flow cytometry. Mean CFSE fluorescence intensities (MFI) for the lymphocyte populations are indicated at the upper left. Differences in apoptosis were quantified by Annexin V labeling. Data are representative of three independent experiments.

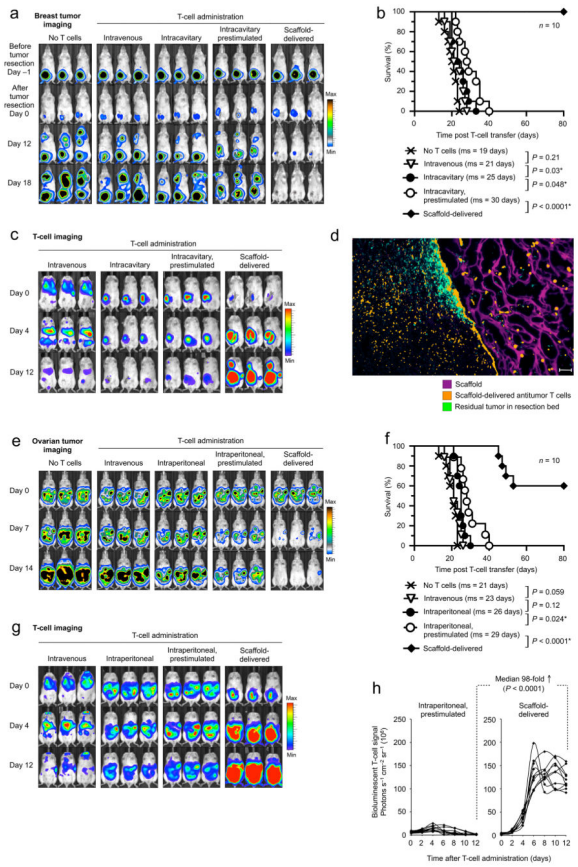

Figure 3.

Material-deployed T cells robustly expand in tumor tissue, where they reduce residual disease and relapse. **(a–d)** Biomaterial-supported T cell implants eradicate tumor cells left behind after surgery. Ten days after firefly luciferase-expressing 4T1 breast tumor cells were transplanted into mammary glands of BALB/c mice, tumors were resected such that ~1% of the tissue remained. All mice were treated with cyclophosphamide one day prior to T cell treatment. The first group of mice received a cell-free scaffold immediately following surgery as a control; all others were treated with 7×10^6 breast tumor-specific T cells. In group 2, the cells were injected intravenously. The next two groups were injected with T cells directly into the tumor bed, with or without pre-activation using anti-CD3/CD28/CD137 antibodies and IL-15/IL-15Rα. The last group received cells delivered via bioactive scaffolds that were implanted directly into the resection cavity. (**a**) Sequential bioluminescence imaging of the 4T1 breast tumors. (**b**) Kaplan-Meier survival curves for treated and control mice. Shown are ten mice per treatment group pooled from three independent experiments; ms, median survival. (**c**) Longitudinal *in vivo* bioluminescence imaging of breast tumor-specific T cells retrovirally transduced with click beetle red luciferase (CBR-luc). (**d**) Tumor-specific T cells labeled with CellTracker Orange were embedded in scaffolds that were fluorescently tagged with Hilyte Fluor 647 and implanted into the luciferase-expressing tumor resection cavity. The scaffold and surrounding tissue were excised and sectioned for histological analysis three days later. Scale bar: 100 μm. Data shown are 1 of 2 independent experiments. (**e–h**) Launching anti-tumor T lymphocytes

from bioactive polymer implants controls inoperable cancer. ID8 ovarian carcinoma cells stably expressing VEGF were injected intraperitoneally and allowed to establish for eight weeks. Mice were given cyclophosphamide one day prior to treatment with lymphocytes expressing chimeric NKG2D receptors (NKG2D CARs) using the administration and stimulation protocols described above (except local injections were intraperitoneal instead of intra-resection cavity). (**e**) Serial *in vivo* bioluminescence imaging of ID8-VEGF-luc tumors. (**f**) Survival of animals following T cell therapy depicted as Kaplan-Meier curves. (**g**) *In vivo* bioluminescent imaging of T cells expressing CBR-luc. (**h**) CBR-luc signal intensities after T cell transfer. Every line represents one animal and each dot reflects the whole animal photon count. Pairwise differences in photon counts between treatment groups were analyzed with the Wilcoxon rank-sum test. Shown are data for ten mice per treatment condition.